Substrate-induced band gap in graphene on hexagonal boron nitride: *Ab initio* density functional calculations

Gianluca Giovannetti,[1,2] Petr A. Khomyakov,[2] Geert Brocks,[2] Paul J. Kelly,[2] and Jeroen van den Brink[1,3]

[1]*Instituut-Lorentz for Theoretical Physics, Universiteit Leiden, P.O. Box 9506, 2300 RA Leiden, The Netherlands*

[2]*Faculty of Science and Technology and MESA+ Institute for Nanotechnology, University of Twente, P.O. Box 217, 7500 AE Enschede, The Netherlands*

[3]*Institute for Molecules and Materials, Radboud Universiteit Nijmegen, P.O. Box 9010, 6500 GL, Nijmegen, The Netherlands*

We determine the electronic structure of a graphene sheet on top of a lattice-matched hexagonal boron nitride (*h*-BN) substrate using *ab initio* density functional calculations. The most stable configuration has one carbon atom on top of a boron atom, and the other centered above a BN ring. The resulting inequivalence of the two carbon sites leads to the opening of a gap of 53 meV at the Dirac points of graphene and to finite masses for the Dirac fermions. Alternative orientations of the graphene sheet on the BN substrate generate similar band gaps and masses. The band gap induced by the BN surface can greatly improve room temperature pinch-off characteristics of graphene-based field effect transistors.

INTRODUCTION

Less than three years ago, it was discovered that graphene—a one-atom-thick carbon sheet—can be deposited on a silicon oxide surface by micromechanical cleavage of high quality graphite.[1] The graphene flakes are micrometers in size, sufficiently large to have contacts attached so as to construct field effect transistors (FETs). Electrical transport measurements made clear that at room temperature, graphene has an electron mobility of at least $10\,000\ \mathrm{cm^2/V\,s}$, a value ten times higher than the mobility of silicon wafers used in microprocessors.[1–3] The high mobility is not much affected by a field-induced excess of electrons or holes.

A graphene sheet has a honeycomb structure with two crystallographically equivalent atoms in its primitive unit cell. Two bands with p_z character belonging to different irreducible representations cross precisely at the Fermi energy at the K and K' points in momentum space. As a result undoped graphene is a zero-gap semiconductor. The linear dispersion of the bands results in quasiparticles with zero mass, so-called Dirac fermions. At energies close to the degeneracy point, the electronic states form perfect Dirac cones. The absence of a gap, preventing the Dirac fermions from attaining a finite mass and complicating the use of graphene in electronic devices,[4] is related to the equivalence of the two carbon sublattices of graphene.

The relativistic nature of the Dirac fermions gives rise to counterintuitive phenomena. One, known as the Klein paradox, is that relativistic electrons exhibit perfect transmission through arbitrarily high and wide potential barriers. This effect is related to an unwanted characteristic of graphene FETs, namely, that pinchoff is far from complete.[5] If one applies a gate voltage so that either holes or electrons are injected into the graphene sheet, the FET is open and its conductivity high. One can then try to block the current by tuning the gate voltage to move the graphene layer toward the charge neutrality point where the Fermi energy coincides with the Dirac points; at this energy, the density of states vanishes and nominally there are no carriers present. How-

ever, it turns out that in spite of the lack of electronic states the conductivity does not vanish in this case. Rather, it assumes the minimal value $\sigma_{\min} = 4e^2/h$, where h is Planck's constant and e the unit of charge. Thus even when pinched off to its maximum the FET still supports an appreciable electrical current, which is intrinsic to graphene and related to the fact that the Dirac fermions are massless.[2–7]

INDUCING A GAP

The poor pinchoff can only be remedied by generating a mass for the Dirac fermions. A number of possibilities exist to do so. One is to use bilayer graphene which will have a gap if the top and bottom layers are made inequivalent, for instance, by applying a bias potential.[5] Another is the use of graphene nanoribbons, where gaps arise from the lateral constriction of the electrons in the ribbon. The size of the gap then depends on the detailed structure of the ribbon edges.[8–10] We investigate an alternative possibility and consider graphene on a substrate that makes the two carbon sublattices inequivalent. This breaks the sublattice symmetry directly, generating an intrinsic and robust mass for the Dirac fermions.

As a substrate, hexagonal boron nitride (*h*-BN) is a suitable choice.[11] This wide gap insulator has a layered structure very similar to that of graphene but the two atoms in the unit cell are chemically inequivalent. Placed on top of *h*-BN the two carbon sublattices of graphene become inequivalent as a result of the interaction with the substrate. Our band structure calculations in the local-density approximation show that a gap of at least 53 meV—an energy roughly twice as large as k_BT at room temperature—is induced. This can be compared to graphene on a copper (111) metallic surface where the gap is found to be much smaller and can even vanish, depending on the orientation of the graphene sheet.

STABLE STRUCTURE

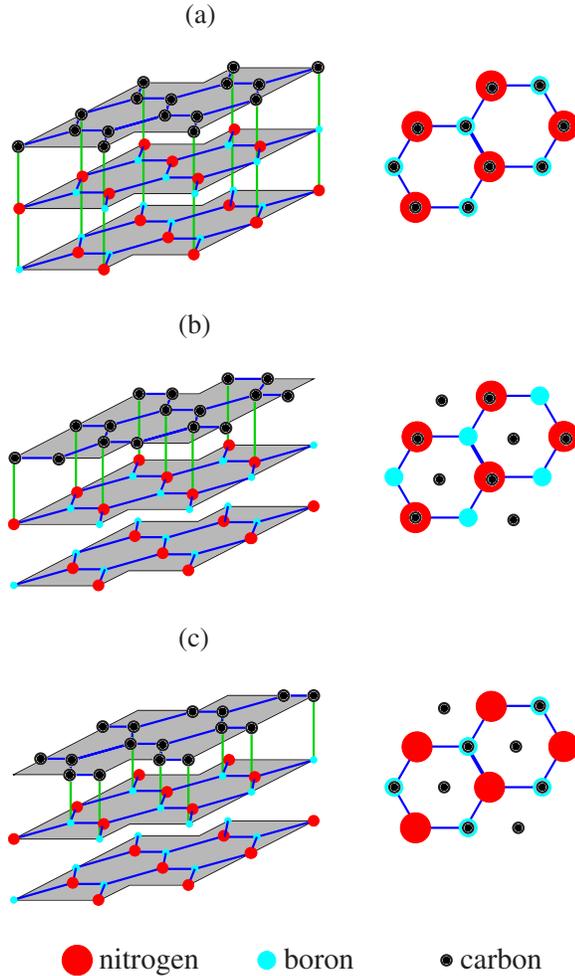The lattice mismatch of graphene with hexagonal boron nitride is less than 2%. Just as in graphite, the interaction

FIG. 1. (Color online) The three inequivalent orientations of single-layer graphene on a h-BN surface. Left, side view; right, top view.

FIG. 2. (Color online) Total energy E of graphene on h-BN surface for the three configurations (a), (b), and (c) as a function of the distance between the graphene sheet and the top h-BN layer.

between adjacent BN layers is weak. The h-BN layers have an AA' stacking: the boron atoms in layer A are directly above the nitrogen atoms in layer A'. Within the local density approximation (LDA), the minimum energy separation of adjacent layers is found to be 3.24 Å, which is reasonably close to the experimental value of 3.33 Å. Because generalized gradient approximation calculations give essentially no bonding between BN planes and lead to excessively large values of c,[12] we opt for electronic structure calculations within the LDA. Electronically, h-BN is a wide gap insulator, with experimentally a gap of 5.97 eV.[13] This gap is underestimated by about 33% in LDA. A quasiparticle GW correction on top of the LDA brings it into very close agreement with experiment[14,15] and reinterprets experiment in terms of an indirect gap. For the composite graphene layer on top of h-BN system, we use the LDA lattice parameter for graphene, $a=2.445$ Å.

On the basis of this structural information, we construct a unit cell with four layers of h-BN and a graphene top layer. We represent the vacuum above graphene with an empty space of 12–15 Å. The results to be presented below converge quickly as a function of the number of h-BN layers and the width of the vacuum space, consistent with weak
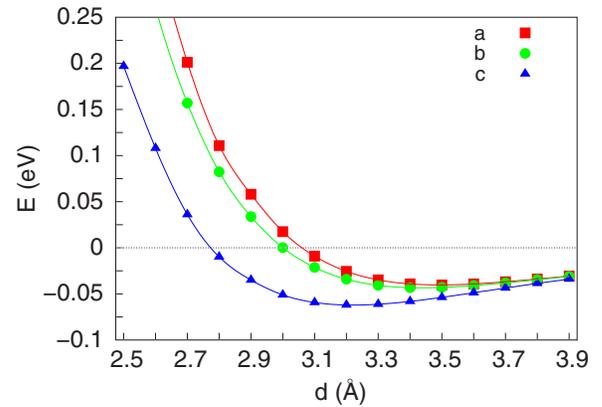
interlayer interactions. No significant difference in the final results was found when six layers of h-BN were used. The in-plane periodicity is that of a single graphene sheet with a hexagonal unit cell containing two carbon atoms. We consider three inequivalent orientations of the graphene sheet with respect to the h-BN, see Fig. 1:

(1) the (a) configuration with one carbon over B, and the other carbon over N:

(2) the (b) configuration with one carbon over N, and the other carbon centered above a h-BN hexagon; and

(3) the (c) configuration with one carbon over B, and the other carbon centered above a h-BN hexagon.

The self-consistent calculations were performed with the Vienna *ab initio* simulation package (VASP)[16,17] using a plane wave basis and a kinetic energy cutoff of 600 eV. The Brillouin zone (BZ) summations were carried out with the tetrahedron method and a $36 \times 36 \times 1$ grid which included the Γ, K, and M points. A dipole correction avoids interactions between periodic images of the slab along the z direction.[18]

The total energies of the three configurations are shown as a function of the distance between the h-BN surface and the graphene sheet in Fig. 2. For all distances, the lowest-energy configuration is (c) with one carbon on top of a boron atom and the other above a h-BN ring. The equilibrium separation of 3.22 Å for configuration (c) is smaller than 3.50 Å for configuration (a) and 3.40 Å for configuration (b). For all three configurations, the energy landscape is seen to be very flat around the energy minimum. Though symmetry does not require inequivalent carbon atoms to be equidistant from the BN layer, in practice the stiffness of the graphene sheet prevents any significant buckling.

BAND STRUCTURE

With the stable structures in hand, we compute the corresponding electronic band structures and projected densities of states which are shown in Fig. 3 for configuration (c). For the h-BN derived bands, a gap of 4.7 eV at the K point is found, which is nearly identical to the LDA gap value at this particular point in the Brillouin zone found for bulk h-BN.[15] Within this boron nitride gap, the bands have entirely carbon
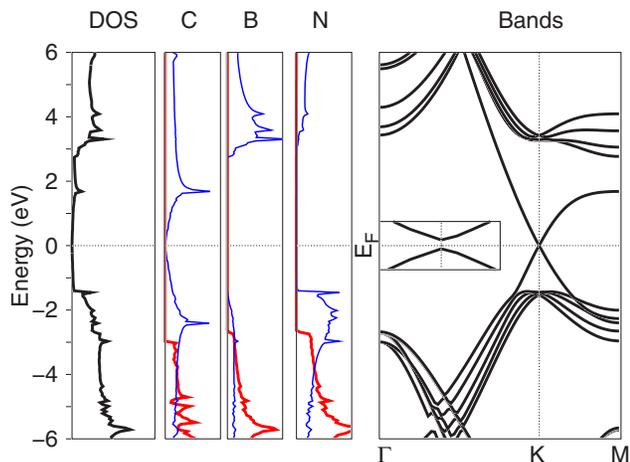
FIG. 3. (Color online) Band structure along the ΓK and KM directions in reciprocal space, and total and projected densities of states (DOSs) for the relaxed structure (c) of graphene on h-BN. Carbon, boron, and nitrogen projected DOSs are shown, with a projection on the p states in plane (red and/or thick gray lines) and out of plane (blue and/or thin gray lines). The inset is a magnification of the bands around the K point, where the gap opens.

character as expected on the basis of the weak interlayer interactions in both bulk h-BN and graphite. On the eV scale of Fig. 3, the Dirac cone around the K point appears to be preserved. However, zooming in on that point in the BZ (see inset) reveals that a gap of 53 meV is opened and the dispersion around the Dirac points is quadratic.

The band gaps for the three different configurations are shown in Fig. 4 as a function of the distance between the graphene sheet and the h-BN surface. Decreasing this distance increases the gap, as expected for a physical picture based upon a symmetry-breaking substrate potential. The band gaps that are opened at the equilibrium geometries of
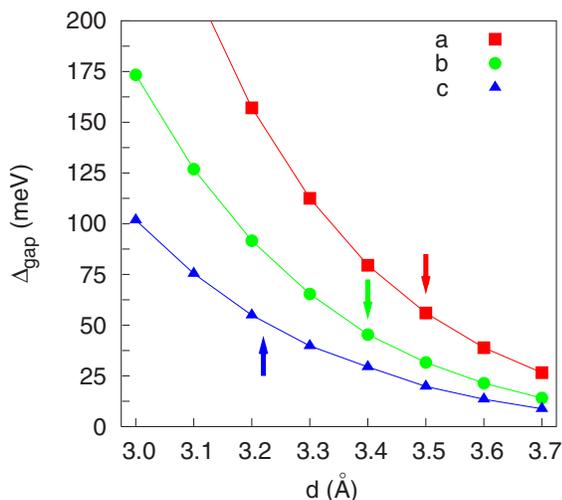

FIG. 4. (Color online) The values of the gaps for the three configurations (a), (b), and (c) as a function of the distance between the graphene sheet and the top h-BN layer. The calculated equilibrium separations are indicated by vertical arrows.

the (a) and (b) configurations are 56 and 46 meV, respectively, which are comparable to the band gap obtained for configuration (c). The largest gap is found for the (a) configuration with one carbon atom above a boron atom and the other above a nitrogen atom. Again, this is expected for gap opening induced by breaking the symmetry of the two carbon atoms. Since LDA generally underestimates the gap, the values that we obtain put a lower bound on the induced band gaps, which we thus find to be significantly larger than k_BT at room temperature.

Although the lattice mismatch between graphene and h-BN constants is less than 2% and can be neglected in a first approximation, in a real system incommensurability will occur and we expect the strong in-plane bonding of both graphene and h-BN to prevail over the weak interplane bonding. For graphene on Ir(111) where the lattice mismatch is ~10%, moiré patterns have been observed in scanning tunneling microscopy images.[19] There, first-principles calculations showed that regions could be identified where the graphene was in registry with the underlying substrate in high symmetry configurations analogous to the (a)–(c) configurations discussed above, and transition regions with little or no symmetry.[19] The graphene separation from the substrate varied across the surface leading to bending of the graphene sheet. If we could take the lattice mismatch into account in a large supercell in a similar fashion, some areas of graphene would be forced into the higher energy (a) and (b) configurations with larger separations to the BN substrate. However, the corresponding band gaps are all of the order of the 50 meV we find for the lowest energy (c) configuration or higher. It seems reasonable to conclude that the lattice mismatch will not reduce the gap substantially.

Cu(111) SUBSTRATE

The situation changes markedly for graphene on a Cu(111) surface. The copper surface layer forms a triangular lattice, matching that of graphene to better than 4%. We consider two configurations of graphene on Cu(111). Either the center of each carbon hexagon is on top of a Cu atom, which we call the symmetric configuration in the following, or every second carbon atom is on top of a Cu atom, which we call the asymmetric configuration. For the asymmetric and symmetric configurations, LDA calculations yield equilibrium separations of 3.3 and 3.4 Å which are comparable to those of graphene on h-BN (Fig. 2). The total energy difference between the two configurations is only about 9 meV. In the asymmetric configuration, a small gap of 11 meV is opened in the graphene band structure, whereas in the symmetric configuration the gap remains very close to zero. In both cases, we find very little mixing between copper and carbon states. The difference between the gaps can be explained by the fact that the symmetric configuration preserves the graphene symmetry in the top Cu surface layer, whereas the symmetry is broken in the asymmetric configuration. The effect of this symmetry breaking is small, however, and the resulting band gap is much smaller than that induced by h-BN and comparable to the typical thermal broadening reported in experiments.[2,4] Taking into account

the graphene-Cu lattice mismatch in, for instance, a supercell calculation[19] will not change this conclusion.

For both configurations of graphene on Cu, a charge rearrangement at the interface is found which moves the Fermi level away from the induced gap[20] by much more than the magnitude of the gap itself. This is in contrast to a h-BN substrate, where the Fermi level remains in the induced gap. Around the Fermi level of graphene on Cu, the band dispersion is still linear. Consequently, the properties characteristic of graphene which result from the linear dispersion should be preserved. In, for instance, tunneling experiments that require adsorption of graphene on a metallic (Cu) substrate,[21] one should still be able to observe the intrinsic linear electronic structure of graphene near the Fermi energy, but no longer at the Dirac points.

CONCLUSIONS

Our density functional calculations show that the carbon atoms of a graphene sheet preferentially orient themselves directly above the boron atoms of a h-BN substrate, with one carbon sublattice above the boron sublattice and the other carbon centered above a h-BN ring. Although graphene interacts only weakly with the h-BN substrate, even when a few angstroms away the presence of h-BN induces a band gap of 53 meV, generating an effective mass for the Dirac fermions of $4.7 \times 10^{-3} m_e$, where m_e is the electron mass. The gap that opens at the Dirac points is considerably larger than the one for graphene on Cu(111). Additional quasiparticle interactions, for instance taken into account within a *GW* scheme, will increase the value of the gap. The opening of a band gap in graphene on h-BN offers the potential to improve the characteristics of graphene-based FETs, decreasing the minimum conductance by orders of magnitude. Other interesting features such as the valley degree of freedom, which is related to the degeneracy of the K and K' points in the Brillouin zone, remain intact and can still be used to control an electronic device.[22] Also the half-integer quantum Hall effect—a peculiar characteristic of graphene—remains unchanged.[2,23,24]

[1] K. S. Novoselov, A. K. Geim, S. V. Morozov, D. Jiang, Y. Zhang, S. V. Dubonos, I. V. Grigorieva, and A. A. Firsov, Science **306**, 666 (2004).

[2] K. S. Novoselov, A. K. Geim, S. V. Morozov, D. Jiang, M. I. Katsnelson, I. V. Grigorieva, S. V. Dubonos, and A. A. Firsov, Nature (London) **438**, 197 (2005).

[3] Y. B. Zhang, Y. W. Tan, H. L. Stormer, and P. Kim, Nature (London) **438**, 201 (2005).

[4] A. K. Geim and K. S. Novoselov, Nat. Mater. **6**, 183 (2007).

[5] M. I. Katsnelson, K. S. Novoselov, and A. K. Geim, Nat. Phys. **2**, 620 (2006).

[6] H. B. Heersche, P. Jarillo-Herrero, J. B. Oostinga, L. M. K. Vandersypen, and A. F. Morpurgo, Nature (London) **446**, 56 (2007).

[7] J. van den Brink, Nat. Nanotechnol. **2**, 199 (2007).

[8] Y. W. Son, M. L. Cohen, and S. G. Louie, Phys. Rev. Lett. **97**, 216803 (2006).

[9] M. Y. Han, B. Ozyilmaz, Y. Zhang, and P. Kim, Phys. Rev. Lett. **98**, 206805 (2007).

[10] Z. Chen, Y.-M. Lin, R. J. Rooks, and P. Avouris, arXiv:cond-mat/0701599.

[11] K. Suenaga, C. Colliex, N. Demoncy, A. Loiseau, H. Pascard, and F. Willaime, Science **278**, 653 (1997).

[12] G. Kern, G. Kresse, and J. Hafner, Phys. Rev. B **59**, 8551 (1999).

[13] K. Watanabe, T. Taniguchi, and H. Kanda, Nat. Mater. **3**, 404 (2004).

[14] X. Blase, A. Rubio, S. G. Louie, and M. L. Cohen, Phys. Rev. B **51**, 6868 (1995).

[15] B. Arnaud, S. Lebegue, P. Rabiller, and M. Alouani, Phys. Rev. Lett. **96**, 026402 (2006).

[16] G. Kresse and J. Furthmuller, Phys. Rev. B **54**, 11169 (1996).

[17] G. Kresse and J. Furthmuller, Comput. Mater. Sci. **6**, 15 (1996).

[18] J. Neugebauer and M. Scheffler, Phys. Rev. B **46**, 16067 (1992).

[19] A. T. N'Diaye, S. Bleikamp, P. J. Feibelman, and T. Michely, Phys. Rev. Lett. **97**, 215501 (2006).

[20] G. Giovannetti, P. A. Khomyakov, G. Brocks, J. van den Brink, and P. J. Kelly (unpublished).

[21] C. Oshima and A. Nagashima, J. Phys.: Condens. Matter **9**, 1 (1997).

[22] A. Rycerz, J. Tworzydlo, and C. W. J. Beenakker, Nat. Phys. **3**, 172 (2007).

[23] N. M. R. Peres, F. Guinea, and A. H. Castro Neto, Phys. Rev. B **73**, 125411 (2006).

[24] V. P. Gusynin and S. G. Sharapov, Phys. Rev. Lett. **95**, 146801 (2005).